ChemComm

View Online
Dynamic Article Links

Cite this: *Chem. Commun.*, 2011, **47**, 4670–4672

www.rsc.org/chemcomm

COMMUNICATION

Molecular engineering of photoresponsive three-dimensional DNA nanostructures†

Da Han,[a] Jin Huang,[ab] Zhi Zhu,[a] Quan Yuan,[a] Mingxu You,[a] Yan Chen[ab] and Weihong Tan*[ab]

Received 15th February 2011, Accepted 28th February 2011
DOI: 10.1039/c1cc10893j

This study demonstrates the use of azobenzene-incorporated DNA as a control agent to precisely monitor three-dimensional DNA nanostructures. The shape of a DNA tetrahedron can be controlled by alternate irradiations with different wavelengths of light.

DNA is a useful construction material for various nanostructures by virtue of the remarkable hybridization specificity between complementary strands. Research on DNA nanostructures has not only improved the understanding of fundamental problems in genetics, but has also generated interest in exploring practical applications.[1] By using smart design, different static DNA nanostructures[2,3] have already been prepared.

Recently, reconfigurable DNA nanostructures capable of three-dimensional movement have attracted increasing interest because of their potential applications in intelligent drug delivery[4] and smart molecular sensing.[5] Active control of three-dimensional movement for DNA structures is usually achieved by input of specific molecular signals, such as DNA strands,[6,7] enzymes[8] or protons,[9] to trigger a change in the shape or size of the structure. However, a major shortcoming arises from those designs because the accumulated DNA output waste can quickly deteriorate device performance and ultimately bring it to a halt.[10] To overcome this problem, a recycled drive power input is highly desired. Compared with other input signals, photons have significant advantages, such as clean, permanently high efficiency and no waste accumulation. In addition, by using light, DNA nanostructures can be remotely controlled, opening novel avenues in nanomedicine. Consequently, a photon-regulated, shape-changing DNA nanostructure would greatly contribute to applications in many fields of nanoscience.

Azobenzene has proven to be an effective photo-sensitive component because of its reversible stereo isomerization from the *trans* to *cis* forms at 300–380 nm and from *cis* to *trans* at wavelengths >400 nm.[11] By incorporating azobenzene moieties into DNA double-stranded structures, hybridization can be controlled by the interconversion of azobenzene between the planar *trans* and nonplanar *cis* forms, allowing the formation of photocontrollable DNA structures.[12,13] Here, we construct a photocontrollable, reconfigurable three-dimensional DNA nanostructure using azobenzene incorporated-DNA.[14–16] The strategy of using azobenzene is universal and can be extended to any type of DNA nanostructure, providing new routes for manipulation of nanoscale shapes using photons.

A previously reported method was used to construct robust DNA tetrahedral structures by an assembly of appropriately designed oligonucleotide sequences.[6,17] Inspired by the contraction and extension of a string, a hairpin structure was incorporated into the DNA tetrahedron. The hairpin can be opened and closed *via* hybridization and dehybridization, as shown in Scheme 1.

DNA sequences S1, S2, S3 and S4 form the contracted DNA tetrahedron with the hairpin in the closed state. Strands S5 with incorporated azobenzene moieties can hybridize with the hairpin portion, allowing the control of open–closed cycles of the hairpin structure by using UV and visible light. To achieve optimal photon-control, four S5 sequences were designed, as shown in Scheme 1. The smallest number of azo moieties is 7 (S5-7Azo), with azobenzene inserted every three bases. Sequences with azobenzenes inserted every two bases (S5-9Azo) and every one base (S5-17Azo) were also synthesized. Considering that the distance of the azobenzene moieties from the sequence ends may influence hybridization efficiency, S5-10Azo was designed with a different azo-moiety distance from the sequence ends compared to S5-9Azo. With UV irradiation, the azobenzene molecules change to the nonplanar *cis* form separating strands S1 and S5, thus forcing the hairpin to form and finally converting the entire structure to the contracted state. On the other hand, when visible irradiation (>450 nm) is applied, the azobenzene molecules convert back to the planar *trans* form and rehybridize with strand S1 to open the hairpin and extend the DNA tetrahedron. In this way, the shape of the entire DNA three-dimensional structure can be precisely controlled by photon irradiation.

Native polyacrylamide gel electrophoresis (PAGE) was used to confirm the formation of azobenzene-incorporated DNA

[a] *Center for Research at Bio/nano Interface, Department of Chemistry and Department of Physiology and Functional Genomics, Shands Cancer Center, University of Florida, Gainesville, Florida 32611-7200, USA*
[b] *State Key Laboratory of Chemo/Biosensing and Chemometrics, College of Biology and College of Chemistry and Chemical Engineering, Hunan University, Changsha 410082, P.R. China. E-mail: tan@chem.ufl.edu; Fax: +86 352 846 2410*

† Electronic supplementary information (ESI) available: Experimental section, materials, and fluorescence measurements. See DOI: 10.1039/c1cc10893j

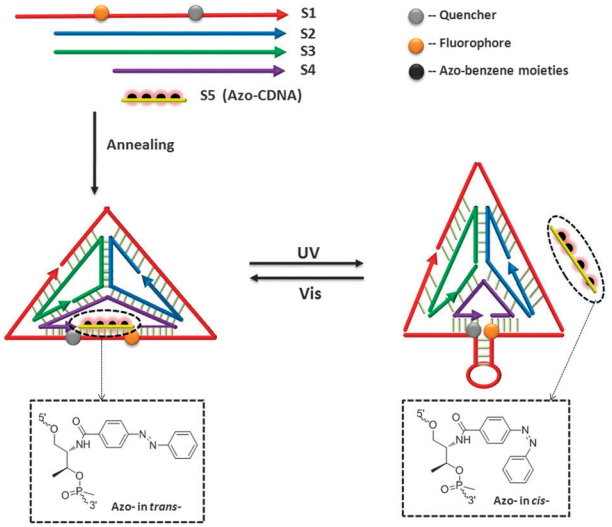

Scheme 1 Photocontrollable DNA nanostructure using azobenzenes. S1, S2, S3, S4 and S5 were mixed in the ratio of 1 : 1 : 1 : 1 : 16 to form the azo-incorporated tetrahedral structures. Four S5 sequences were designed with different azobenzene moiety numbers. S5-7Azo, S5-9Azo, S5-10Azo and S5-17Azo contain 7, 9, 10 and 17 azobenzene moieties, respectively. A fluorophore and a quencher were incorporated at the ends of the hairpin to indicate structural movement.

tetrahedra. As demonstrated by Goodman *et al.*,[6] the contracted tetrahedral structures (T1) form by combining equal amounts of strands S1, S2, S3 and S4, giving a total base pair number of 125. If S5 without azobenzenes is included, the hairpin in T1 is completely opened and forms the extended structure (T2). Structures T-7Azo, T-9Azo, T-10Azo and T-17Azo were formed by mixing S5-7Azo, S5-9Azo, S5-10Azo and S5-17Azo with the other four strands, respectively.

The gel result in Fig. 1 shows that the azobenzene-incorporated tetrahedral structures (from lanes 3 to 6) can form the extended tetrahedral structures under visible irradiation compared with T1 (Lane 1) and T2 (Lane 2). However, some contracted structures also appeared along with the extended forms, and they became more and more obvious as the number of azobenzene moieties increased, indicating that hybridization efficiency is affected by the azobenzene moieties. The four azo-incorporated structures

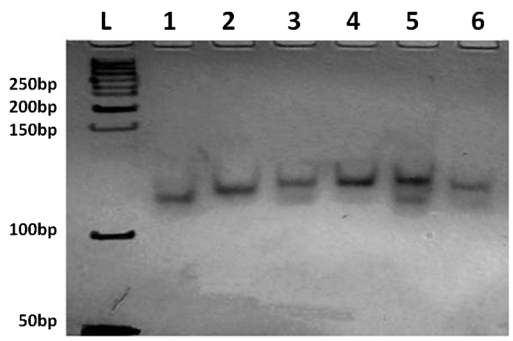

Fig. 1 Native polyacrylamide gel electrophoresis (6%) analysis of different azo-incorporated tetrahedral structures at 4 °C. Lane 1 corresponds to the contracted tetrahedron without S5. Lane 2 is the extended tetrahedron with S5-cDNA (no azobenzenes). Lanes 3–6 are the bands of T-7Azo, T-9Azo, T-10Azo and T-17Azo, respectively. L: 50bp ladder consisting of double strands of DNA with length increase in 50bp steps.

have slightly lower mobilities than T2 because the azo moieties increase the molecular weight of the structures compared with T2. Thus, in the presence of azobenzene-incorporated strands, the DNA tetrahedral structures can still be successfully constructed. AFM images of T-10Azo were also obtained to visualize the structures (see ESI†, Fig. S1).

Fluorescence measurements were used to demonstrate the photo-control of the Azo-DNA tetrahedral structures. Fluorophores (FAM) and quenchers (Dabcyl) were incorporated at the two ends of the hairpins in S1. When the tetrahedron is in the contracted state, the fluorescence is quenched as a result of the close proximity of FAM and Dabcyl. When the hairpin is opened to form the extended structure, the fluorescence intensity should increase by the separation of fluorophores and quenchers. Fluorescence signals of structures T1 and T2 were used to obtain the background and maximum signals, respectively. In Fig. 2a, when UV irradiation was applied to T-10Azo, the fluorescence intensity decreased because the dehybridization of azo-incorporated S5 strands promoted the formation of hairpin structures. Different azobenzene-incorporated structures were tested at 48 °C, and their fluorescence signals were normalized based on the maximum signal of T2 (Fig. 2b). The results showed that tetrahedral structures containing a low percentage of azobenzenes (T-Azo7) did not respond differentially to either UV or visible light, indicating that S5 did not dissociate effectively from the structures. On the other hand, structures possessing the maximum number of azobenzenes (*e.g.*, T-Azo17) showed poor hybridization between S5 and S1, even under visible irradiation. Based on these findings, we concluded that the structures containing one azobenzene between every two nucleotides in S5 (*i.e.*, T-Azo9 and T-Azo10) give the best photon response efficiency and optimum structural stability.

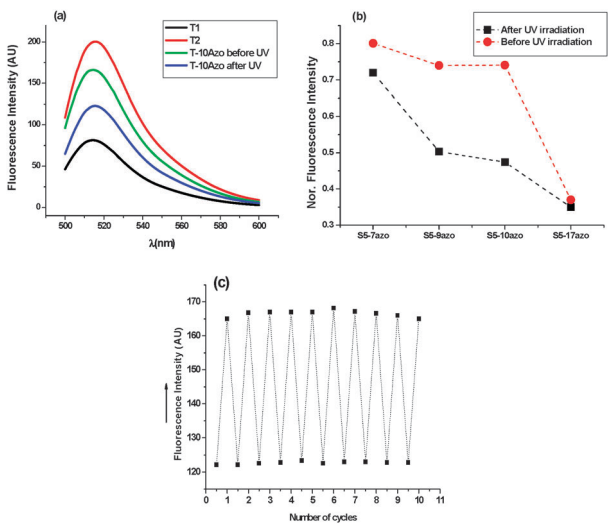

Fig. 2 (a) Fluorescence measurement of T-10Azo labeled with FAM and Dabcyl in response to UV irradiation. T1 is the contracted tetrahedral structure without strand 5; T2 is the completely extended tetrahedral structure with cDNA (no azobenzenes). (b) Fluorescence signal differences in response to UV irradiation for different azo-incorporated tetrahedral structures. (c) Cycling of the closed–open forms at 48 °C by repeated visible (λ = 450 nm) and UV (λ = 350 nm) irradiations for 3 min each (λ_{exc} = 488 nm; λ_{em} = 515 nm).

Fig. 2c shows the fluorescence changes as the T-10Azo structures extended and contracted with successive irradiation by UV (3 min) and visible light (3 min). The efficiency did not decrease, even after 10 open/closed iterations with no addition of extra oligonucleotides and no generation of waste strands. Therefore, this photon-regulated DNA structure is stable and robust. Additionally, all the cycles were performed at 48 °C in order to have rapid dynamic response to the wavelength changes. Here, the melting temperatures of S5-10Azo and S1 in the *cis* and *trans* configurations are 30.1 °C and 55.7 °C, respectively, and the photon-fueled reconfigurable structures work most efficiently at around 45–55 °C. The relatively high experimental temperature is the reason for the relatively high background signal. Overall, these results demonstrated successful, long-lasting control of structural alternation with photon energy input.

To visualize the structural changes when applying different wavelengths of light, gold nanoparticles were assembled with tetrahedral structures. Taking advantage of Au-NPs' uniform size, clear visualization by TEM, and site-specific control on DNA strands by using phosphorothioate DNA and bifunctional linkers,[18] gold nanoparticles (diameter of 3.5 nm) were attached at the three vertices of the variational triangular face of the tetrahedral structures (Scheme 2). For further details of the assembly method, please see ESI.† When the shapes of the tetrahedron change, the relative positions of particles at the vertices of the triangle change accordingly. This method allowed clear visualization of the movement of DNA structures triggered by light. In Fig. 3a, the sizes of extended structures matched well with the calculated values. The two isosceles edges are around 7 nm, and the bottom edge is 11 nm long. After UV irradiation, some tetrahedra converted to contracted structures, causing the bottom edges of triangles to shrink to 4 nm, as shown in Fig. 3b.

To remove the interference of random alignment of AuNPs, control experiments were also performed. For the DNA tetrahedral structures without any phosphorothioate modification, no regular triangular structures were found in the TEM image (Fig. 3c). These images were consistent with the fluorescence data and demonstrated the successful working mechanism of our photon-regulated reconfigurable DNA nanostructures.

In summary, we have successfully used azobenzenes to construct a tetrahedral DNA nanostructure controlled by photons. PAGE and AFM were utilized to confirm the existence of the tetrahedral DNA nanostructures. Fluorescence

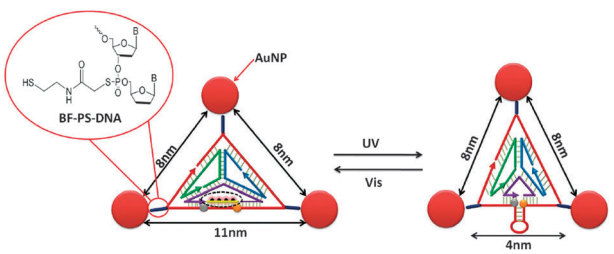

Scheme 2 Illustration of gold nanoparticle (AuNP) assembly at three vertices of the variational triangular faces of tetrahedra by a phosphorothioate anchor and a short bifunctional fastener (BF). AuNPs can be attached to the BF-PS-DNA sites to observe different triangular shapes under UV and visible irradiation.

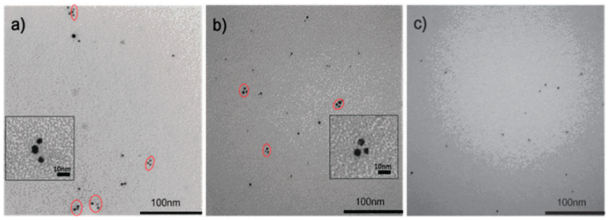

Fig. 3 TEM images of AuNPs assembled at three vertices of the variational triangular face of tetrahedra. (a) Before UV irradiation. (b) After UV irradiation. (c) Tetrahedra without any phosphorothioate modifications are shown as control.

intensity changes, as well as AuNP-assisted TEM measurements, demonstrated the photon-controllability. These results indicate that incorporation of azobenzene moieties into DNA strands allows control of the three-dimensional structure, in line with our previous report[16] which demonstrated the control of a two-dimensional DNA hairpin structure. We believe that this work will open doors to implement and facilitate the study of conversion of solar energy to kinetic energy. One potential application is the utilization of the 3-D structural changes to trigger the release of cargos (such as proteins or other macromolecules) encapsulated in the DNA nanostructure, as a smart drug delivery system with precise temporal and spatial resolution.

We thank the NIH for supporting this work. This work was also supported by the National Key Scientific Program of China (2011CB911000) and China National Grand Program on Key Infectious Disease (2009ZX10004-312).

Notes and references

1 N. C. Seeman, *Trends Biochem. Sci.*, 2005, **30**, 119–125.
2 N. C. Seeman, *J. Theor. Biol.*, 1982, **99**, 237–247.
3 J. Malo, J. C. Mitchell, C. Venien-Bryan, J. R. Harris, H. Wille, D. J. Sherratt and A. J. Turberfield, *Angew. Chem., Int. Ed.*, 2005, **44**, 3057–3061.
4 F. Tanaka, T. Mochizuki, X. G. Liang, H. Asanuma, S. Tanaka, K. Suzuki, S. Kitamura, A. Nishikawa, K. Ui-Tei and M. Hagiya, *Nano Lett.*, 2010, **10**, 3560–3565.
5 G. Seelig, D. Soloveichik, D. Y. Zhang and E. Winfree, *Science*, 2006, **314**, 1585–1588.
6 R. P. Goodman, M. Heilemann, S. Doose, C. M. Erben, A. N. Kapanidis and A. J. Turberfield, *Nat. Nanotechnol.*, 2008, **3**, 93–96.
7 B. Yurke, A. J. Turberfield, A. P. Mills, F. C. Simmel and J. L. Neumann, *Nature*, 2000, **406**, 605–608.
8 J. Bath, S. J. Green and A. J. Turberfield, *Angew. Chem., Int. Ed.*, 2005, **44**, 4358–4361.
9 D. S. Liu and S. Balasubramanian, *Angew. Chem., Int. Ed.*, 2003, **42**, 5734–5736.
10 F. C. Simmel and W. U. Dittmer, *Small*, 2005, **1**, 284–299.
11 G. S. Kumar and D. C. Neckers, *Chem. Rev.*, 1989, **89**, 1915–1925.
12 H. Asanuma, T. Ito, T. Yoshida, X. G. Liang and M. Komiyama, *Angew. Chem., Int. Ed.*, 1999, **38**, 2393–2395.
13 X. G. Liang, T. Mochizuki and H. Asanuma, *Small*, 2009, **5**, 1761–1768.
14 H. Asanuma, X. Liang, H. Nishioka, D. Matsunaga, M. Liu and M. Komiyama, *Nat. Protoc.*, 2007, **2**, 203–212.
15 X. G. Liang, H. Nishioka, N. Takenaka and H. Asanuma, *ChemBioChem*, 2008, **9**, 702–705.
16 H. Z. Kang, H. P. Liu, J. A. Phillips, Z. H. Cao, Y. Kim, Y. Chen, Z. Y. Yang, J. W. Li and W. H. Tan, *Nano Lett.*, 2009, **9**, 2690–2696.
17 R. P. Goodman, I. A. T. Schaap, C. F. Tardin, C. M. Erben, R. M. Berry, C. F. Schmidt and A. J. Turberfield, *Science*, 2005, **310**, 1661–1665.
18 J. H. Lee, D. P. Wernette, M. V. Yigit, J. Liu, Z. Wang and Y. Lu, *Angew. Chem., Int. Ed.*, 2007, **46**, 9006–9010.

